Supplementary Information (SI) for Inorganic Chemistry Frontiers.

A Solvent Free Neutral Co Complex Exhibiting Macroscopic Polarization Switching Induced by Directional Charge Transfer

Zi-Qi Zhou,[†] Shu-Qi Wu,[†,‡] Qi-Rui Shui,[†] Wen-Wei Zheng,[†] Akari Maeda,[†] Xiao-Peng Zhang,[†] Jing Chu,[†] Shinji Kanegawa,[†,‡] Sheng-Qun Su,[†,‡]and Osamu Sato*[,†,‡]

[†]*Institute for Materials Chemistry and Engineering, Kyushu University.*

Motooka, Nishi-ku, Fukuoka 819-0395, Japan

[‡]*IRCCS, Integrated Research Consortium on Chemical Sciences, Kyushu University.*

*E-mail: sato@cm.kyushu-u.ac.jp

Table of Contents

1. Experimental Procedures

Reagents.

Dicobalt octacarbonyl ($Co_2(CO)_8$, 98%), Catechol and N,N,N',N'-Tetraethylethane-1,2-diamine (teeda) were purchased from Tokyo Chemical Industry, Japan. 1.0 mol/L Titanium tetrachloride ($TiCl_4$, 99%) in toluene was purchased from Sigma-Aldrich, 37% Formalin, Toluene and other solvents were purchased from Wako Pure Chemical Industries, Ltd., Japan. 3,6-di-tert-butyl-1,2-benzoquinone were prepared using by the reported method.

Synthesis.

Single crystals of **[Co(teeda)(3,6-dbq)$_2$]** were obtained by a mild method. First, the starting Co^{II}_4(3,5-dbsq)$_8$ was synthesized. Dicobalt octacarbonyl was dissolved and stirred in 25 ml toluene in a nitrogen gas atmosphere. After 15 minutes, a 25 ml solution of 3,6-di-tert-butyl-1,2-benzoquinone which was dissolved in the toluene was slowly injected into the dicobalt octacarbonyl solution with a 1 ml injector for 25 times. The mixture of reaction lasted for 30 minutes and let it stand overnight. Dark green micro crystals were collected and dried after filtration. Secondly, Co^{II}_4(3,5-dbsq)$_8$ was added into a 25 ml toluene solvent and stirring in N_2 gas atmosphere. After ten minutes, 10 ml toluene solution of teeda was slowly added into the Co solution with a 1 ml injector. The reaction was stirred at room temperature for 30 minutes and remove solution in a vacuum pressure. Black powder of crude products was formed and collected with 92% yield based on 3,6-di-tert-butyl-1,2-benzoquinone. For growing single large crystals to measure physical properties, 80 mg powder of **[Co(teeda)(3,6-dbq)$_2$]** was dissolved in hot toluene and filtered hot solution three times. After remove the air in solutions the solutions were evaporated in slowly flowed N_2 atmosphere. After 1 week, large block crystals were crystalized with 78% yield based on teeda. Elemental analysis result: H, 9.57%; C, 67.52%, N, 3.98%, which is in a good agreement with theoretical result: H, 9.601%; C, 67.933%, N, 4.169%.

Single-Crystal X-ray Diffraction.

Single-crystal X-ray diffraction data of **[Co(teeda)(3,6-dbq)$_2$]** were collected on a Rigaku XtaLAB Synergy R, DW system, HyPix four-circle diffractometer equipped with a Rigaku (Mo) X-ray Source. The data reduction was integrated with the program CrysAlisPro 1.171.42.72a (Rigaku OD, 2022). Their structures were solved with a direct method by using the SHELXT 2018/2 (Sheldrick, 2018) and refined by the SHELXL 2018/3 (Sheldrick, 2015) *in* Olex2 1.5 (Dolomanov et al., 2009) *program*. Their structures were checked by PLATON and no higher symmetries and solvents were suggested. [1-3] CCDC ***2348589*** for 250 K and CCDC ***2348587*** for 100 K CCDC ***2379769*** for 150K, CCDC ***2069770*** for 350K, CCDC ***2069771*** for 200K and CCDC ***2369772*** for 300K**.** The details of crystal data can be acquired free of charge via www.ccdc.cam.ac.uk/datarequest/cif.

Powder X-ray Diffraction Pattern

Powder x-ray diffraction pattern measurement was performed on the Rigaku Rint TTR III with a Cu Kα radiation at room temperature. The data was collected in the 2θ range of 5-50° with 1.5°/min scan

speed and step width of 0.02°.

IR Spectroscopy.

The infrared absorption spectra were recorded between 1600 cm^{-1} and 1200 cm^{-1} with KBr pellets on a FT/IR-660 plus (Jasco) spectrophotometer.

Thermal Analysis.

Thermogravimetric analysis (TGA) was measured from room temperature to 300 °C with a heating rate of 10 °C min^{-1} in the air on a DTU-2A equipment.

UV–Vis–NIR Absorption Spectroscopy.

The Ultraviolet–visible (UV-Vis) absorption spectroscopy was collected using a UV-3100PC (Shimadzu) scanning spectrophotometer.

Supplementary Theoretical Calculation.

In the computation for the **[Co(teeda)(3,6-dbq)$_2$]**, Gaussian 09 (Revision D.01) package was used in which the B3LYP functional was used for all energy calculations. For the Co, H, C, N, and O atoms, the 6-311+G* basis set was also used. Molecular structures were adopted as the initial guess.[4-8] The dipole moment results at doublet and sextet were calculated by DFT method and symmetry turned off by external request for consistent with crystalline axis.The molecular structures of the doublet and sextet states were also optimized with the B3LYP functional but with 6-311G basis set, which provided similar results. After geometry optimizations, vibrational analyses were performed to ensure that no imaginary frequencies were found, and the calculated IR spectra based on the frequency analysis were in good agreement with the experimental results, indicating the reliability of the optimized geometries. For UV-vis spectra calculation, TDDFT with nstates = 30 was used. Spin density map were carried on the gaussian view with a of the density envelope is 0.025 $Å^{-3}$.

Table S1. Crystal data and structure refinements for **[Co(teeda)(3,6-dbq)$_2$]** at 100 K and 350 K.

Empirical formula	100K	150K	200K	250K	300K	350K
Formula weight	671.84	671.84	671.84	671.84	671.84	671.84
Temperature (K)	100(2)	150(2)	200(2)	249.98(11)	300(2)	350(2)
Crystal color	Dark blue	Dark blue	Dark blue	Dark blue	Dark blue	Dark blue
Wavelength (Å)	0.71073	0.71073	0.71073	0.71073	0.71073	0.71073
Crystal system	Orthorhombic	Orthorhombic	Orthorhombic	Orthorhombic	Orthorhombic	Orthorhombic
Space group	$Pna2_1$	$Pna2_1$	$Pna2_1$	$Pna2_1$	$Pna2_1$	$Pna2_1$
a / Å	20.0783(9)	20.2540(8)	20.3540(7)	20.4554(8)	20.4713(9)	20.5581(9)
b / Å	10.0110(5)	10.1648(4)	10.2865(4)	10.3488(4)	10.3296(5)	10.3902(5)
c / Å	18.7804(8)	18.7069(6)	18.6663(5)	18.7372(6)	18.7315(9)	18.7856(7)
Volume/ Å^3	3774.9(3)	3851.3(2)	3908.2(2)	3966.5(2)	3961.0(3)	4012.6(3)
Z	4	4	4	4	4	4
ρ_{calcd} / g·cm^{-3}	1.182	1.159	1.142	1.125	1.127	1.112
μ / mm^{-1}	0.493	0.484	0.477	0.470	0.470	0.464
F(000)	1460.0	1460.0	1460.0	1460.0	1460.0	1460.0
2θ range	5.038 to 54.968	4.984 to	4.944 to	4.918 to	4.924 to	4.898 to 54.97
Reflections	38800/8514	40364/8822	42096/8943	43090/9078	47901/9065	43739/9196
Completeness	99.8%	99.8%	99.7%	99.7%	99.7%	99.8%
Goodness	1.032	1.043	1.029	1.025	1.065	1.017
R_1,WR_2	0.0368, 0.0951	0.0443/0.1167	0.0402/0.1046	0.0423, 0.1084	0.0510, 0.1356	0.0474, 0.1187
R_1,WR_2	0.0409, 0.0975	0.0504/0.1196	0.0455/0.1070	0.0490, 0.1116	0.0604, 0.1418	0.0608, 0.1253
Largest diff, peak	0.43/-0.22	0.64/-0.28	0.50/-0.23	0.44/-0.21	0.39/-0.18	0.38/-0.19

[a] $R_1 = \Sigma||F_o| - |F_c||/\Sigma|F_o|$ and $wR_2 = [\Sigma w(Fo^2 - Fc^2)^2/ \Sigma w\ F_o4]^{1/2}$.

Table S2. Atomic coordinates, equivalent isotropic displacement parameters (Å^2) of **[Co(teeda)(3,6-dbq)$_2$]** at 100 K.

Atom	***Wyck.***	***x***	***y***	***z***	U_{eq}[a]
Co1	4a	0.56723(2)	0.45349(3)	0.53872(2)	0.01939(10)
O1	4a	0.51988(11)	0.3528(2)	0.46674(11)	0.0263(5)
O2	4a	0.62375(9)	0.29995(19)	0.54243(13)	0.0253(4)
O3	4a	0.62158(11)	0.5207(2)	0.46459(11)	0.0210(4)
O4	4a	0.63017(12)	0.5377(2)	0.60155(12)	0.0241(5)
N1	4a	0.50722(11)	0.6249(2)	0.53627(17)	0.0267(5)
N2	4a	0.50319(14)	0.3826(3)	0.62006(14)	0.0277(6)

[a]U_{eq} is defined as 1/3 of the trace of the orthogonalized U_{ij} tensor.

Table S3. Atomic coordinates, equivalent isotropic displacement parameters (Å^2) of **[Co(teeda)(3,6-dbq)$_2$]** at 250 K.

Atom	***Wyck.***	***x***	***y***	***z***	U_{eq}[a]
Co1	4a	0.56613(2)	0.55030(3)	0.54009(3)	0.03377(11)
O1	4a	0.52298(10)	0.6620(2)	0.46236(11)	0.0422(5)
O2	4a	0.62484(9)	0.71238(19)	0.54151(14)	0.0446(4)
O3	4a	0.62682(13)	0.4749(2)	0.46398(12)	0.0413(5)
O4	4a	0.63582(12)	0.4652(2)	0.60290(12)	0.0395(5)
N1	4a	0.50136(11)	0.3784(2)	0.53875(18)	0.0427(5)
N2	4a	0.49804(14)	0.6194(3)	0.62458(15)	0.0451(6)

[a]U_{eq} is defined as 1/3 of the trace of the orthogonalized U_{ij} tensor.

Table S4. Anisotropic displacement parameters (Å^2) of **[Co(teeda)(3,6-dbq)$_2$]** at 100 K.

Atom	U_{11}	U_{22}	U_{33}	U_{12}	U_{13}	U_{23}
Co1	0.01991(16)	0.02151(17)	0.01675(16)	0.00069(12)	-0.00033(17)	-0.00109(18)
O1	0.0209(10)	0.0327(12)	0.0253(10)	-0.0038(9)	-0.0007(8)	0.0008(9)
O2	0.0240(8)	0.0288(9)	0.0232(9)	0.0021(7)	-0.0005(10)	0.0011(10)
O3	0.0218(10)	0.0235(11)	0.0175(9)	0.0024(8)	-0.0024(8)	-0.0014(8)
O4	0.0269(12)	0.0268(11)	0.0185(10)	0.0006(8)	-0.0016(9)	-0.0038(8)
N1	0.0289(11)	0.0273(11)	0.0241(11)	0.0000(9)	0.0001(13)	0.0030(13)
N2	0.0340(15)	0.0266(14)	0.0226(12)	0.0018(11)	-0.0002(10)	0.0032(10)

Table S5. Anisotropic displacement parameters (Å^2) of **[Co(teeda)(3,6-dbq)$_2$]** at 250 K.

Atom	**U_{11}**	**U_{22}**	**U_{33}**	**U_{12}**	**U_{13}**	**U_{23}**
Co1	0.03296(18)	0.03516(19)	0.03318(17)	-0.00116(13)	-0.00103(18)	0.0028(2)
O1	0.0391(11)	0.0464(13)	0.0410(11)	0.0014(10)	-0.0052(9)	0.0023(9)
O2	0.0445(10)	0.0460(11)	0.0433(9)	-0.0057(8)	-0.0092(12)	0.0052(12)
O3	0.0453(13)	0.0459(14)	0.0329(10)	-0.0027(10)	-0.0027(9)	0.0024(9)
O4	0.0377(12)	0.0463(14)	0.0346(10)	0.0014(9)	-0.0002(9)	0.0058(9)
N1	0.0425(12)	0.0408(12)	0.0447(11)	-0.0052(9)	-0.0017(14)	-0.0015(15)
N2	0.0463(15)	0.0471(17)	0.0418(13)	-0.0034(12)	0.0045(12)	-0.0035(11)

Table S6. Selected bond lengths (Å**)** and angles (deg.) for **[Co(teeda)(3,6-dbq)$_2$]** at 100 K.

Co(1)-O(1)	1.936(2)	Co(1)-O(4)	1.923(2)
Co(1)-O(2)	1.9119(19)	Co(1)-N(1)	2.097(2)
Co(1)-O(3)	1.893(2)	Co(1)-N(2)	2.119(3)
C(1)-O(1)	1.324(4)	C(2)-O(2)	1.301(4)
C(3)-O(3)	1.333(4)	C(4)-O(4)	1.343(4)
O(1)-Co(1)-O(2)	84.16(10)	O(2)-Co(1)-O(4)	86.55(9)
O(1)-Co(1)-O(3)	87.40(9)	O(3)-Co(1)-O(4)	85.22(9)
O(1)-Co(1)-O(4)	168.30(10)	O(1)-Co(1)-N(1)	97.39(10)
O(2)-Co(1)-O(3)	88.31(9)	O(1)-Co(1)-N(2)	91.78(9)
O(2)-Co(1)-N(1)	178.41(10)	O(2)-Co(1)-N(2)	93.72(10)
O(3)-Co(1)-N(1)	91.39(10)	O(3)-Co(1)-N(2)	177.73(10)
O(4)-Co(1)-N(1)	91.86(10)	O(4)-Co(1)-N(2)	95.92(10)
N(1)-Co(1)-N(2)	86.62(11)		

Table S7. Selected bond lengths (Å**)** and angles (deg.) for **[Co(teeda)(3,6-dbq)$_2$]** at 250 K.

Co(1)-O(1)	2.059(2)	Co(1)-O(4)	2.048(2)
Co(1)-O(2)	2.063(2)	Co(1)-N(1)	2.219(2)
Co(1)-O(3)	2.045(2)	Co(1)-N(2)	2.227(3)
C(1)-O(1)	1.295(4)	C(2)-O(2)	1.287(4)
C(3)-O(3)	1.286(4)	C(4)-O(4)	1.301(4)
O(1)-Co(1)-O(2)	78.58(9)	O(2)-Co(1)-O(4)	86.38(9)
O(1)-Co(1)-O(3)	88.92(9)	O(3)-Co(1)-O(4)	79.29(9)
O(1)-Co(1)-O(4)	161.21(9)	O(1)-Co(1)-N(1)	100.75(10)
O(2)-Co(1)-O(3)	88.04(10)	O(1)-Co(1)-N(2)	93.12(10)
O(2)-Co(1)-N(1)	178.93(9)	O(2)-Co(1)-N(2)	95.37(10)
O(3)-Co(1)-N(1)	92.79(10)	O(3)-Co(1)-N(2)	176.31(10)
O(4)-Co(1)-N(1)	94.44(10)	O(4)-Co(1)-N(2)	99.49(10)
N(1)-Co(1)-N(2)	83.82(11)		

Table S8. The local dipole moments (μ_x, μ_y and μ_z) in Debye for **[Co(teeda)(3,6-dbq)$_2$]** at 100 K.

	μ_x	μ_y	μ_z
Co^{III}(teeda)(3,6-dbcat)(3,6-dbsq)	-6.6765	1.2824	3.0795
Co^{III}(teeda)(3,6-dbcat)(3,6-dbsq)	6.6765	1.2824	3.0795
Co^{III}(teeda)(3,6-dbcat)(3,6-dbsq)	-6.6765	-1.2824	3.0795
Co^{III}(teeda)(3,6-dbcat)(3,6-dbsq)	6.6765	-1.2824	3.0795
Total	0	0	12.318

Table S9. The local dipole moments (μ_x, μ_y and μ_z) in Debye for **[Co(teeda)(3,6-dbq)$_2$]** at 250 K.

	μ_x	μ_y	μ_z
Co^{II}(teeda)(3,6-dbsq)$_2$	-4.3642	-1.6716	2.4295
Co^{II}(teeda)(3,6-dbsq)$_2$	4.3642	-1.6716	2.4295
Co^{II}(teeda)(3,6-dbsq)$_2$	-4.3642	1.6716	2.4295
Co^{II}(teeda)(3,6-dbsq)$_2$	4.3642	1.6716	2.4295
Total	0	0	9.718

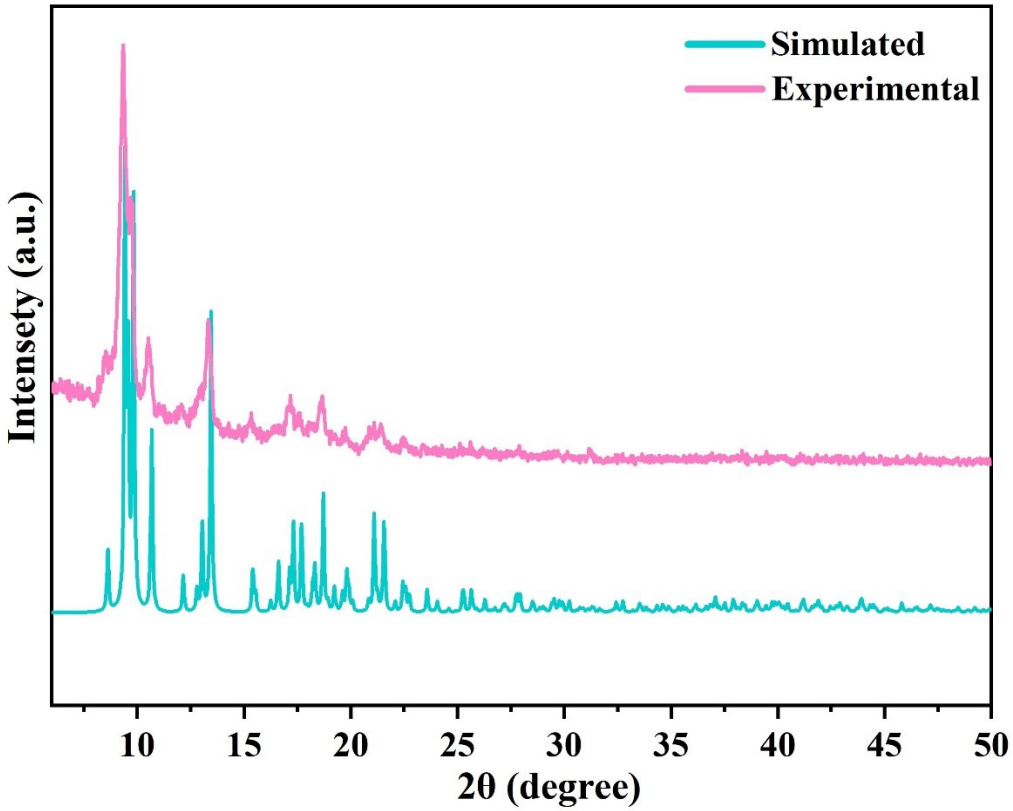

Figure S1. Powder x-ray diffraction pattern of **[Co(teeda)(3,6-dbq)$_2$]**.

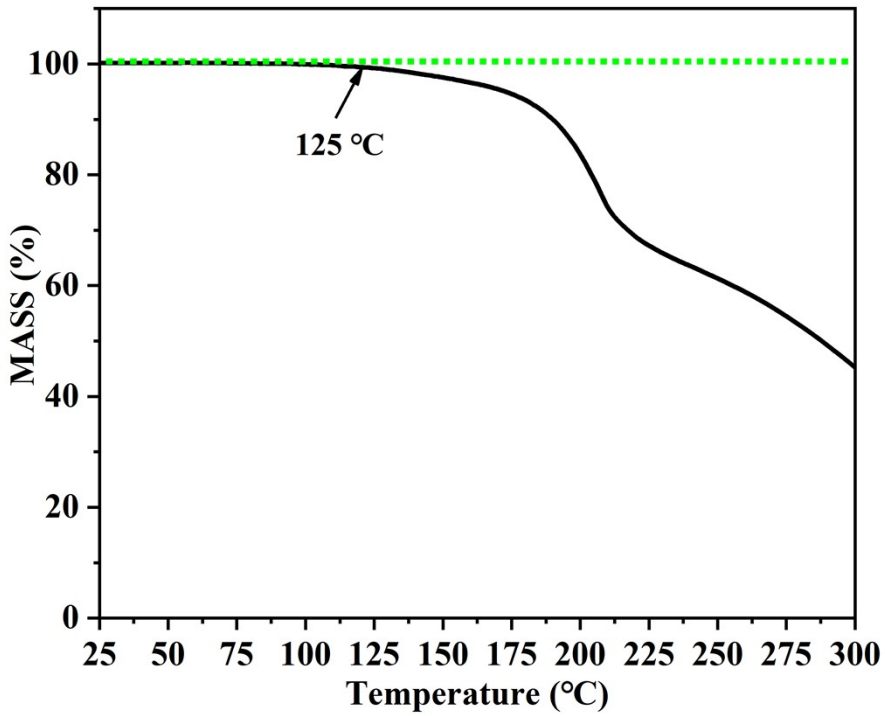

Figure S2. Thermalgravimetric analysis of **[Co(teeda)(3,6-dbq)$_2$]**.

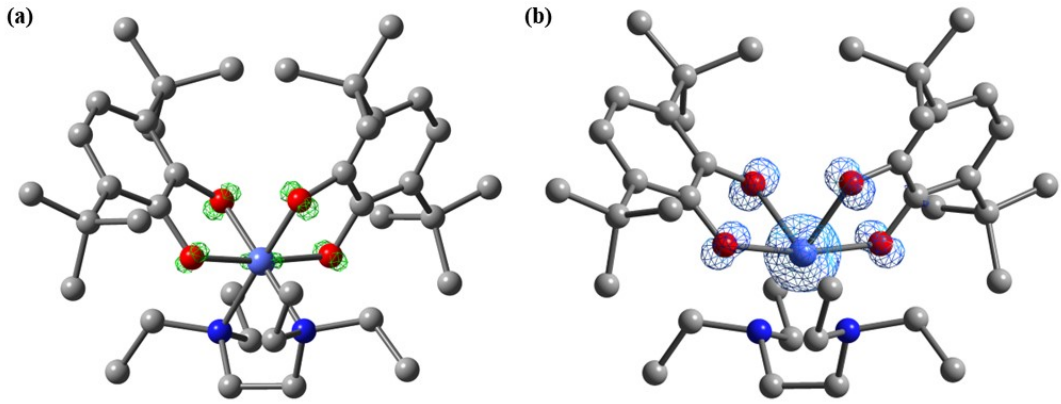

Figure S3. DFT calculation result of spin density in Gaussian View. (a) Doublet spin state. (b) Sextet spin state. Hydrogen atoms were omitted for clarity.

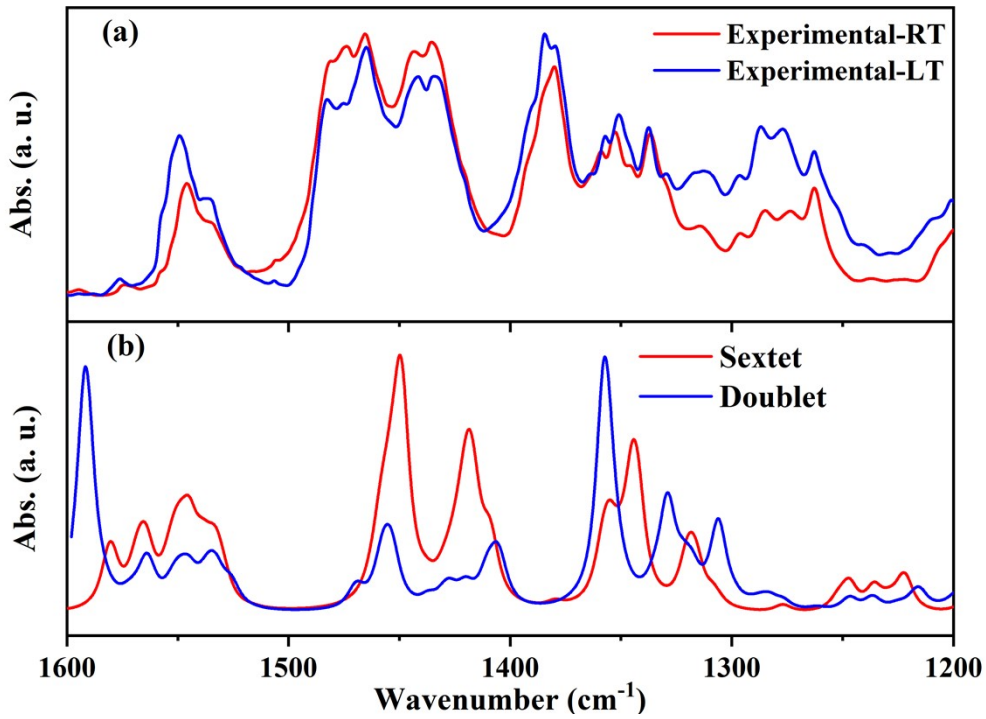

Figure S4. (a) Experimental IR absorption spectra**. (b)** The calculated absorption spectra for the doublet and sextet states.

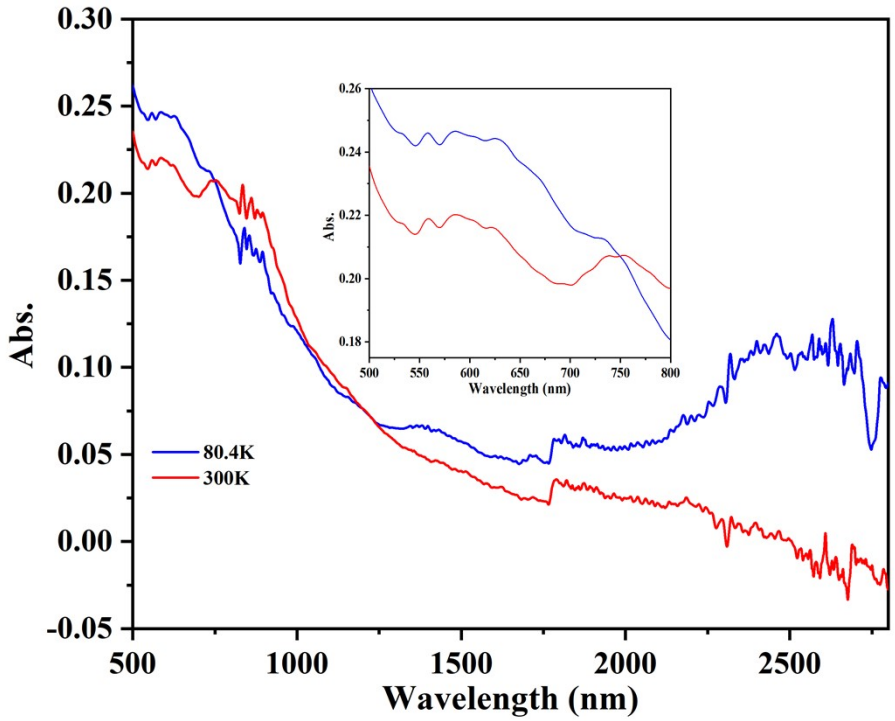

Figure S5. Temperature dependent UV-Vis spectra at 300 K and 80.4 K. Inset: expanded spectra from 500-800 nm.

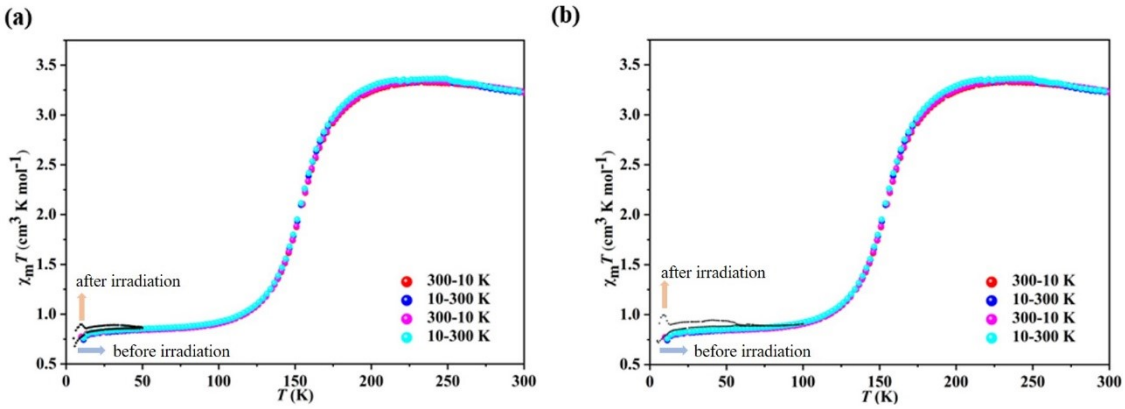

Figure S6. Photo-induced valence tautomerism effect induced by laser at 532 nm (a) and 660 nm (b).

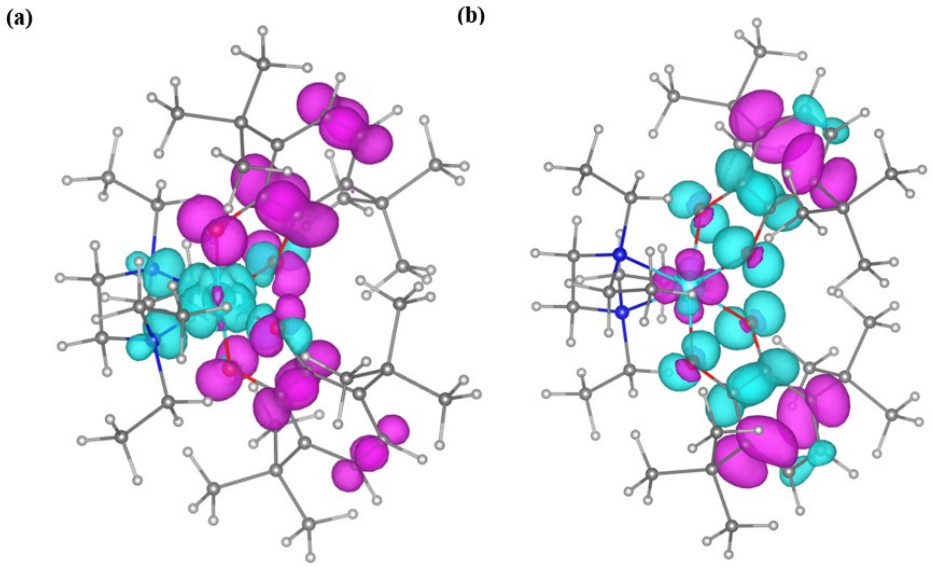

Figure S7. Charge density difference between excited states and ground states in the closed-shell doublet state [$Co^{III\text{-}LS}$(teeda)(3,6-dbsq)(3,6-dbcat)] for transition at 545 nm (a) and the sextet state [$Co^{II\text{-}HS}$(teeda)$(3,6\text{-dbsq})_2$] for transition at 535 nm (b). The contour value of the density envelope is 0.0015 $Å^{-3}$**.** Above results were calculated by multiwfn and drawed by Vesta.

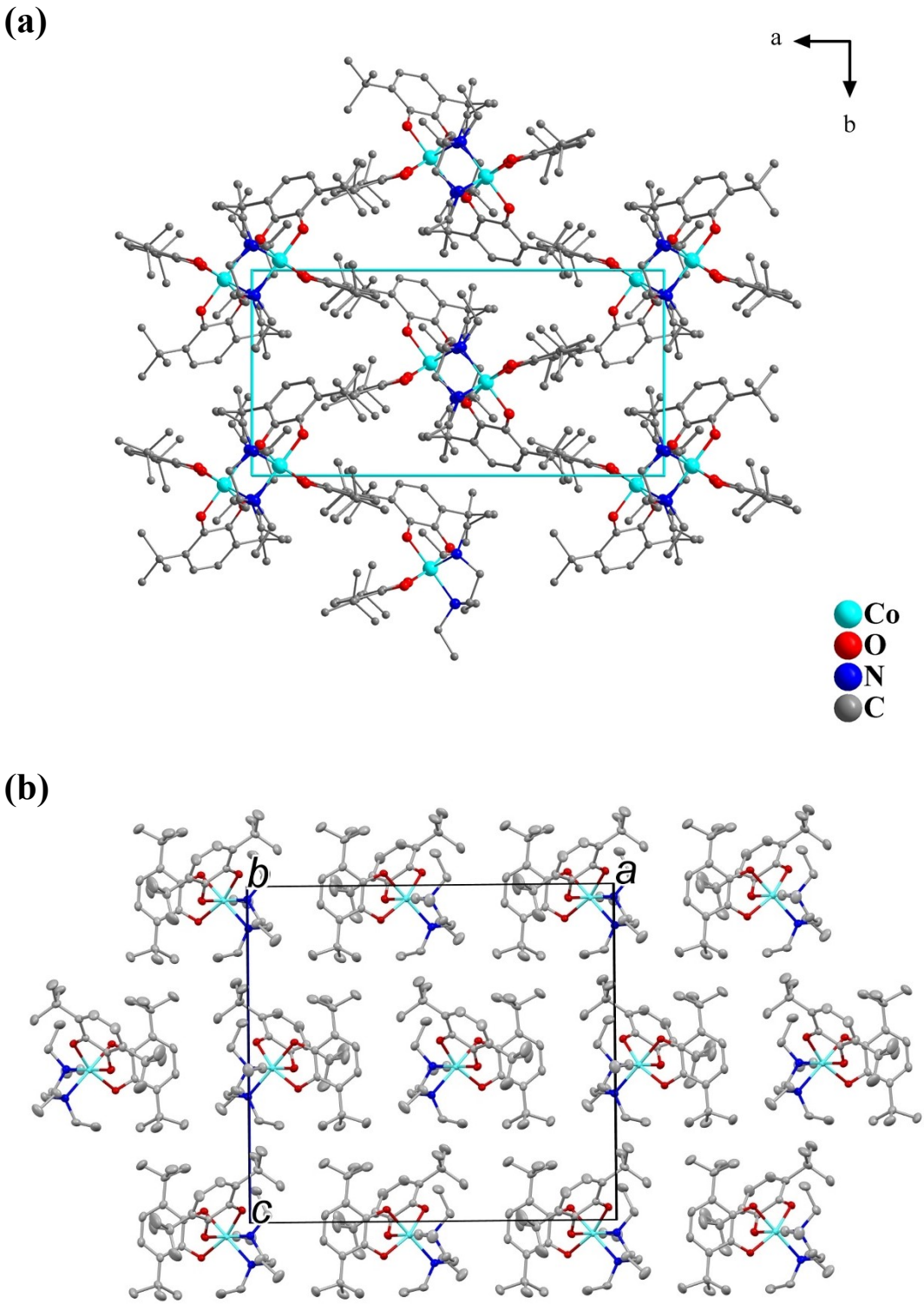

Figure S8. Crystal structure at 100 K in ab plane (a) and ac plane (b). Hydrogen atoms were omitted for clarity.

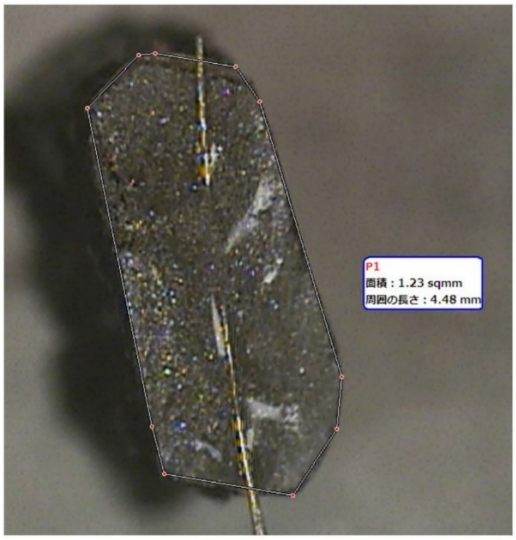

Figure S9. The single crystal to measure pyroelectric currents. The surface that is perpendicular to the c axis is coated with silver paste and gold line. The area of the surface is 1.23 mm^2.

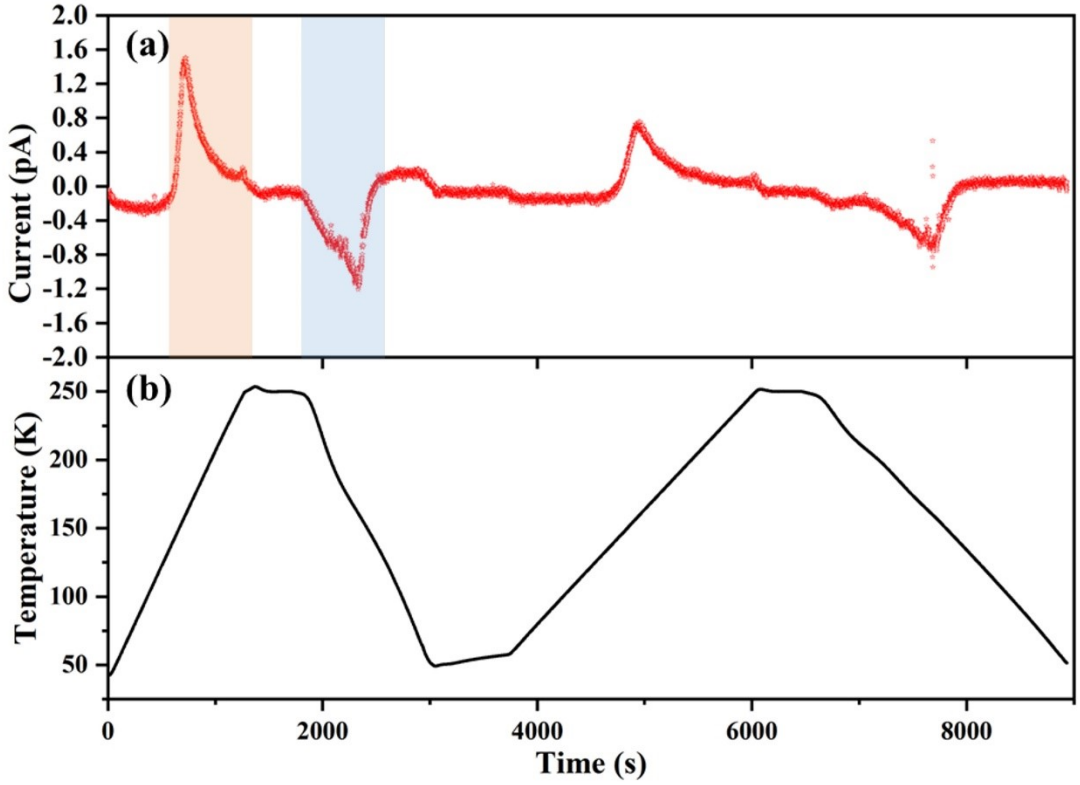

Figure S10. Pyroelectric currents measurement in the MPMS-XL chamber. Panels (a) and (b) show the pyroelectric current and temperature, respectively. We started the measurements after the background noise current was stable. The scan rates in the first and second cooling-heating cycles are 10 and 5 K min^{-1}, respectively.

Reference

1. Sheldrick, G. M. A short history of SHELX. *Acta Crystallogr.* A, **2008**, 64, 112–122.
2. Sheldrick, G. M. Crystal structure refinement with SHELXL. *Acta Crystallogr.C*, **2015**, 71, 3–8.
3. Dolomanov, O. V. et al. OLEX2: a complete structure solution, refinement and analysis program. *J. Appl. Cryst.,* **2009**, 42, 339–341.
4. Frisch, M. et al. Gaussian09. Rev. D.01 (Gaussian, Inc, Wallingford, CT, **2009**).
5. Reiher, M. Theoretical study of the $Fe(phen)_2(NCS)_2$ spin-crossover complex with reparametrized density functionals. *Inorg. Chem.,* **2002**, 41, 6928–6935.
6. Becke, A. D. Density-functional thermochemistry. III. The role of exact exchange. *J. Chem. Phys.,* **1993**, 98, 5648–5652.
7. Lee, C., Yang, W. & Parr, R. G. Development of the Colle-Salvetti correlation energy formula into a functional of the electron density. *Phys. Rev. B,* **1998**, 37, 785.
8. Krishnan, R., Binkley, J. S., Seeger, R. & Pople, J. A. Self-consistent molecular orbital methods. XX. A basis set for correlated wave functions. *J. Chem. Phys*. **1980**, 72, 650–654.